



CATALYTIC OXIDATION OF 2-NITROPHENOL IN WATER OVER Fe(III), Co(II) AND Ni(II) ANCHORED MCM-41

Vishal J. Mayani¹, Krishna Gopal Bhattacharyya², Suranjana V. Mayani*³

¹*Hansgold India Research & Innovation Center (HINDRIC), Hansgold Enviro-catalyst Applied Research Laboratory, Rajkot 360004, Gujarat, India*

²*Department of Chemistry, Gauhati University, Guwahati 781014, Assam, India*

³*Department of Chemistry, Marwadi University, Rajkot-Morbi Road, P.O. Gauridada, Rajkot 360003, Gujarat, India,*

*For correspondence. (suranjana.mayani@marwadieducation.edu.in)

Abstract: Common biological treatments are not very efficient in removing persistent pollutants from water, such as 2-nitrophenol. Oxidation to harmless constituents is the preferred method of treatment. 2-nitrophenol enters water from dyes, pesticides, plasticizer explosives and solvent industries. This paper describes the use of Fe(III), Co(II) and Ni(II) supported MCM-41 as catalysts for oxidizing 2-nitrophenol in water. Oxidation was carried out in the presence and absence of H₂O₂ and the effects of reaction time, mole ratio, catalyst load, reactant concentration, temperature, and pH were evaluated. The conversions achieved for Fe(III), Co(II) and Ni(II) anchored MCM-41 were 47.8, 50.4 and 52.2 % in the presence of H₂O₂ and 39.8, 55.8 and 58.8 % in the absence of H₂O₂, respectively (temperature 353 K, time 300 min, catalyst load 2 g L⁻¹, 2-nitrophenol 10⁻³ M). The preparation of the catalysts and their characterization by atomic absorption spectrometry (AAS), cation exchange capacity (CEC), X-ray diffraction (XRD), Fourier transform infrared spectroscopy (FT-IR), scanning electron microscopy (SEM), thermo gravimetric analysis (TGA) and nitrogen adsorption measurements is described. The oxidation process followed first order kinetics. Some of the oxidation products were identified by gas chromatography mass spectrometry and a probable mechanism is proposed.

Keywords: 2-nitrophenol; Fe(III)-MCM-41; Co(II)-MCM-41; Ni(II)-MCM-41; kinetics; wet oxidation

1. Introduction:

The degradation of phenol and its derivatives have been studied widely over the last few years to develop an efficient process [1-4]. Aromatic nitro compounds are usually resistant to chemical or biological oxidation and to hydrolysis because of the electron-withdrawing nitro group, which makes them environmentally persistent. Remediation of waste streams and ground water contaminated with the phenols is often a difficult task and there is a growing demand for effective, economic and environmentally friendly way to deal with them using processes and materials which are completely benign to the environment. Most nitrophenols are released into the environment during their manufacturing and processing [5-6]. Because of their harmful nature, the U.S. Environmental Protection Agency has listed nitrophenols as pollutant materials. They have also been stated as poisonous for aquatic life and cause odor problems in water tanks [7-8]. 2-Nitrophenol is used mainly to make dyes, paint coloring, rubber chemicals and substances that kill molds. They are also formed in auto exhaust. Effluents from the textile industry may also release both 2-nitrophenol and 4-nitrophenol into surface water. Additionally, the two nitrophenols are found in treated wastewaters from iron and steel manufacturing, foundries, pharmaceutical manufacturing and electrical/electronic components production industries. Both 2-nitrophenol and 4-nitrophenol are detected in the wastewater of a petroleum refining industry [9, 10]. Nitrophenols have also been identified in primary and secondary effluents of municipal waste water treatment plants. The general population may be exposed to nitrophenols through the inhalation of ambient air and ingestion of contaminated foods and drinking water. Destructive processes such as advanced oxidation are currently favored by virtue of their applicability in mineralizing organics to harmless final products [4, 11-15]. Although nitrophenols can be decomposed or oxidized using chemical, photochemical and biological processes, these processes have various disadvantages. The biological processes need longer retention time and are not applicable to high concentrations of pollutants. The chemical methods are additive processes, which are high cost and increase the dissolved solid content in the effluent [16, 17]. Transition metals in various forms are well known oxidizing agents for organic compounds in homogeneous processes. Metal ions or fine particles of the



oxides dispersed in the reaction medium to ensure maximum specific surface area usually constitute the catalyst. If due to some reason, the finely dispersed particles aggregate into bigger ones, there is a rapid loss of surface area and hence, the catalytic activity. This problem is usually overcome by dispersing the catalyst components on a porous support. The well known mesoporous material, MCM-41, has found use as an inert support for oxidation catalysts. MCM-41 [18] has the advantage of a well-defined array of uniform hexagonal mesopores systematically adjustable in the range 1.6-10 nm where various metal species can be incorporated isomorphously. These materials have been proposed as effective catalysts for selective oxidation of organic compounds [19, 20]. Current research focuses on the synthesis and application of modified mesoporous MCM-41 materials, which have an active species attached to the framework via host-guest interactions, creating discrete and uniform catalyst sites on the inner walls of the porous systems [21, 22]. Attempts to insert elements, such as Ti, Cr, Mn and Fe into the MCM-41 framework have met with various degrees of success and use of these materials for catalyzing a number of oxidation reactions in liquid phase has been reported [22, 23].

The present work illustrates the preparation and characterization of Fe(III)-MCM-41(C1), Co(II)-MCM-41 (C2) and Ni(II)-MCM-41(C3) and utilization of these mesoporous materials for wet oxidation of 2-nitrophenol (2-NP) in water. The effectiveness of the catalysts was evaluated with respect to the presence or absence of H₂O₂ as an oxidizing agent in relation to the influence of reaction time, catalyst load and reactant concentration, mole ratio of H₂O₂ with respect to 2-NP, temperature and pH, etc.

2. Experimental:

Material and Methods:

2.1. Chemicals:

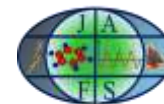
Commercially available aluminum sulphate (Al₂(SO₄)₃·18H₂O, E. Merck, India), sodium hydroxide (NaOH, E. Merck, India), tetramethylammonium hydroxide pentahydrate (TMAOH, Fluka, Switzerland), silica fumed (SiO₂, Sigma, U.S.A), hexadecyl trimethylammonium chloride (HDTMACl, Fluka, Switzerland) were used for synthesizing the support, MCM-41. Iron(III) nitrate nonahydrate (E. Merck, India), cobalt(II) nitrate hexahydrate (E. Merck, India) and nickel(II) nitrate (E. Merck, India) were used for incorporation of the metal cations into MCM-41. 2-nitrophenol (2-NP) for the reactions is procured from Fluka, Switzerland. All other chemicals used are of analytical grade.

2.2. Synthesis of Fe(III), Co(II) and Ni(II) incorporated MCM-41:

MCM-41 was synthesized [24] by mixing together aqueous solutions of aluminium sulphate (0.62 g) and sodium hydroxide (0.3 g) dissolved in minimum volume of water in a 250 ml Teflon-lined beaker and stirring the same continuously till a clear solution was obtained. Tetramethyl ammonium hydroxide (9.4 g) and fumed silica (9.26 g) were added under stirring condition at room temperature. This was followed by slow addition of hexadecyltrimethylammonium chloride (10.55 g) and the pH of the mixture was maintained at 11.0 by adding sodium hydroxide pellets. Stirring was continued till a fine gel of the composition: 1.0 SiO₂: 0.27 HDTMACl: 0.06 Al₂(SO₄)₃ 18H₂O: 0.03 Na₂O: 0.33 TMAOH: 20 H₂O was obtained. The gel was transferred into an autoclave and was kept at 373 K for 24 h. The crystals of MCM-41 were recovered by filtration, washed with deionized water, dried in air and calcined at 823 K in air for 5 h. Fe(III), Co(II) and Ni(II) impregnated MCM-41 materials were prepared by mixing together equal amounts of MCM-41 and iron(III) nitrate nonahydrate or cobalt(II) nitrate hexahydrate or nickel(II) nitrate, using minimum volume of water for wetting, followed by evaporation of the solvent and calcination at 773~873 K for 5 h in air in a muffle furnace.

2.3. Characterization of the catalyst:

MCM-41 synthesis was confirmed by XRD measurements of the prepared sample (Phillips X'pert MPD diffractometer, Almelo, The Netherlands) using Cu anode and comparing the same with known XRD patterns of MCM-41. The percentage of Fe(III), Co(II) and Ni(II) entering into MCM41 was determined with atomic absorption spectrophotometry (Varian SpectrAA220). The functional groups were identified with FTIR measurements (Perkin Elmer Spectrum RXI, range 4400-440 cm⁻¹) using KBr self supported pellet technique. The morphology of the catalysts was measured by scanning electron microscopy (LEO-1430 VP, UK). Thermal stability of the catalysts was determined by thermogravimetric analysis (Mettler Toledo equipment, Model TGA/SDTA 851e, USA), surface area and pore size by nitrogen adsorption-desorption (Micromeritics ASAP-



2010, USA) and cation exchange capacity by copper bisethylenediamine complex method [25].

2.4. Oxidation of 2-NP:

Catalytic oxidation was carried out in a high-pressure stirred reactor (Toshniwal Instruments, India) with equal volumes (25 mL each) of 2-NP and H₂O₂ (concentration 10⁻³ M each), catalyst load of 2 g L⁻¹ at 353 K under an autogenous pressure of 0.2 MPa and stirrer speed of 180 rpm for 5 h. When evaluating the effects of a particular variable, appropriate changes were made in the values of the variable. When no H₂O₂ was used, the total volume was kept at 50 mL. The effects of temperature and pH were studied in a batch reactor. The pH of the 2-NP solution was varied from 3.0 to 8.0 by adding a few drops of 0.1 N HCl or 0.1 N NaOH.

After the reaction was over, the mixture was centrifuged and the unconverted reactant was estimated in the supernatant layer spectrophotometrically (Hitachi U3210). Each reaction was repeated thrice and the mean of the three readings (which were not much different from one another) was reported here. While determining the concentration of the unconverted 2-NP from λ_{\max} measurement, necessary care was taken for the likely interferences from oxidation products and necessary background correction was made in each measurement.

Product identification was done with GC-MS (Shimadzu GC 2010, USA) using Rtx 5 column [packing material: poly (5 % diphenyl 95 % dimethyl) silanone] of length 30 m, diameter 0.25 mm and film thickness 0.25 μ m under temperature programmed mode from 313 to 513K (36 min). At temperature 313 K, hold time was 3.00 min, after which temperature was increased at the rate of 5 K per min to 393 K, which was held for 1.00 min. The rate of increase of temperature was then changed to 20 K per min to the final temperature 513 K, with a hold time of 10 min.

3. Results and Discussion:

3.1. Characterization of the catalysts:

3.1.1. Atomic absorption spectrometry (AAS):

In the impregnation procedure, 0.1 g of MCM-41 and 0.1 g of water soluble salt of the metal (containing 0.014 g Fe(III), 0.020 g Co(II) and 0.020 g Ni(II) in 0.1 g of salt) were taken and the actual amount of metal that entered into MCM-41 was found to be Fe(III): 3.55 mg g⁻¹, Co(II): 19.08 mg g⁻¹ and Ni(II): 22.03 mg g⁻¹ from AAS measurements indicating only 0.36 % Fe(III), 1.91 % Co(II) and 2.20 % Ni(II) (by weight) in the impregnated MCM-41 samples. Since impregnation was carried out by taking equal amounts of MCM-41 and water soluble salt, it is reasonable to compare their catalytic performance.

3.1.2. X-ray diffraction (XRD):

The uncalcined MCM-41 had a prominent peak at $2\theta = 2.45^\circ$ ($d = 36.06 \text{ \AA}$) followed by peaks at 4.15° ($d = 21.27 \text{ \AA}$) and 4.72° ($d = 18.71 \text{ \AA}$). The calcined MCM-41 gave three XRD peaks (Figure 1) corresponding to 2θ values of 2.48° ($d = 35.57 \text{ \AA}$), 4.23° ($d = 20.88 \text{ \AA}$) and 4.93° ($d = 17.91 \text{ \AA}$). Liepold et al. [26] have shown that MCM-41 gives three to five reflections between 20 and 50. The materials are thus expected to have long range order due to hexagonal arrays of parallel silica tubes and are indexed as (100), (110), (200), (210) and (300) reflections. The XRD pattern for the uncalcined MCM-41 at 2.45° , 4.15° and 4.72° corresponding to (100), (110), (200) reflections confirm correct synthesis of MCM-41 in the present work.

The calcined MCM-41 yielded the most prominent diffraction peak at $2\theta = 2.48^\circ$, which could be attributed to (100) reflection, the two other peaks at 4.23° and 4.93° correspond to (110) and (200) reflections. MCM-41 materials are not known to be crystalline at the atomic level, and therefore, no reflections at higher angles are expected. The other reason for this is likely to be due to the structural features having very little influence on reflections at higher angles and even if such reflections exist, they are essentially very weak to be of any significance.

In the XRD patterns of Fe(III)-MCM-41 (C1), Co(II)-MCM-41 (C2), and Ni(II)-MCM-41 (C3) (Figure 1), the prominent (100), (110) and (200) reflections occurred at the 2θ values of Fe(III)-MCM-41: 2.18° ($d = 40.42 \text{ \AA}$), 3.77° ($d = 23.41 \text{ \AA}$), 4.33° ($d = 20.37 \text{ \AA}$), Co(II)-MCM-41: 2.57° ($d = 34.30 \text{ \AA}$), 4.35° ($d = 20.29 \text{ \AA}$), 5.04° ($d = 17.53 \text{ \AA}$) and Ni(II)-MCM-41: 2.54° ($d = 34.69 \text{ \AA}$), 4.33° ($d = 20.38 \text{ \AA}$), 4.94° ($d = 17.86 \text{ \AA}$).

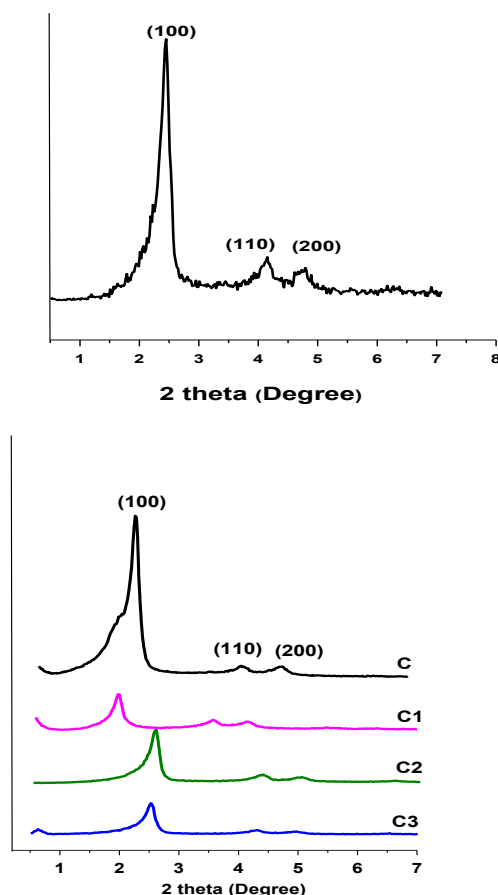


Figure 1: XRD pattern of uncalcined MCM-41 (top) and calcined MCM-41, Fe(III)-MCM-41 (C1), Co(II)-MCM-41 (C2) and Ni(II)-MCM-41 (C3) (bottom).

All the reflection bands suffered shift in case of the catalysts compared to the support, MCM-41 and therefore, metal-incorporation had considerable influence on the structural regularity of the MCM-41 materials. No uniformity could however be noticed in this influence, as was also observed by other workers [22, 27-29].

3.1.3. Fourier transform infrared spectroscopy (FT-IR):

IR spectra of uncalcined MCM-41 and calcined, dehydrated MCM-41 and Fe(III), Co(II) and Ni(II) impregnated MCM-41 showed the prominent IR bands. The bands around 960, 965, 966, 964 and 967 cm^{-1} were observed in uncalcined MCM-41, calcined MCM-41, Co(II)-MCM-41, Ni(II)-MCM-41 and Fe(III)-MCM-41, which are usually assigned to lattice defect and are correlated with the presence of tetrahedral framework ions of M-O-Si type. By carefully examining these bands, a slight red shift in the metal incorporated samples could be detected. Literature suggests that this band can also be assigned to Si-O vibration in Si-OH groups in siliceous MCM-41 [30]. If this is the case, it is reasonable to attribute the red shift in metal incorporated MCM-41 to the replacement of an OH group by O-M type linkage. The broad absorption between 3650 and 3400 cm^{-1} in the FTIR spectra (3430, 3434, 3447, 3450, and 3460 cm^{-1} respectively for uncalcined MCM-41, calcined MCM-41, Fe(III)-MCM-41, Co(II)-MCM-41, and Ni(II)-MCM-41) may be attributed to hydrogen-bonded vicinal pairs of silanol groups [26]. Another broad band appearing in the materials from 1000 to 1250 cm^{-1} (1100 to 1210 cm^{-1} in uncalcined MCM-41, 1090 to 1206 cm^{-1} in calcined MCM-41, 1090 to 1199 cm^{-1} in Fe(III)-MCM41, 1089 to 1219 cm^{-1} in Co(II)-MCM-41, and 1083 to 1219 cm^{-1} in Ni(II)-MCM-41) may be assigned to the asymmetric stretching of Si-O-Si bridges.

The following additional IR bands were also observed: (i) 799, 794, 802, 797 and 799 cm^{-1} , (ii) 1630, 1637,

1648, 1648 and 1646 cm^{-1} respectively for uncalcined MCM-41, calcined MCM-41, Fe(III)-MCM41, Co(II)-MCM-41, and Ni(II)-MCM-41, (iii) 2923, 2930, 2920 and 2925 cm^{-1} respectively for uncalcined MCM-41, Fe(III)-MCM-41, Co(II)-MCM-41, and Ni(II)-MCM-41. These may be attributed to aliphatic C-H bending and stretching vibrations arising from the template [31].

3.1.4. Scanning electron microscopy (SEM):

The SEM images of calcined MCM-41, Fe(III)-MCM-41(C1), Co(II)-MCM-41(C2), and Ni(II)-MCM-41(C3) were given in Figures 2 and 3. The morphology of Fe(III), Co(II) and Ni(II)-MCM-41 was found to be different from that of the parent mesoporous material. The grains of the salts could be clearly seen distributed over the MCM-41 particles in all the three catalysts. No significant difference could be observed between Fe(III)-MCM-41 and Co(II)-MCM-41 with respect to morphology but Ni(II)-MCM-41 showed a slightly different morphology with the salt grains having some preferential distribution.

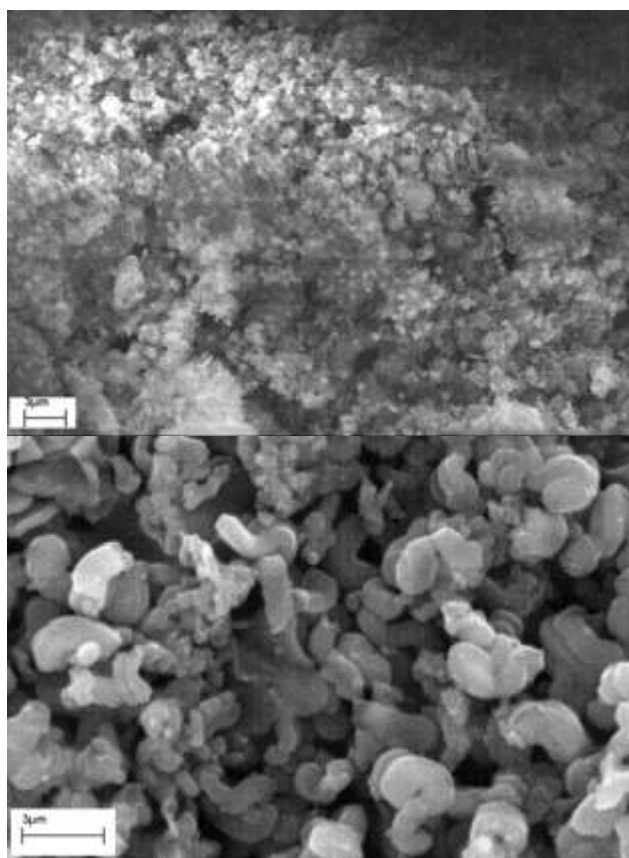


Figure 2: SEM photograph of calcined MCM-41 (top) and Fe(III)-MCM-41 (bottom).

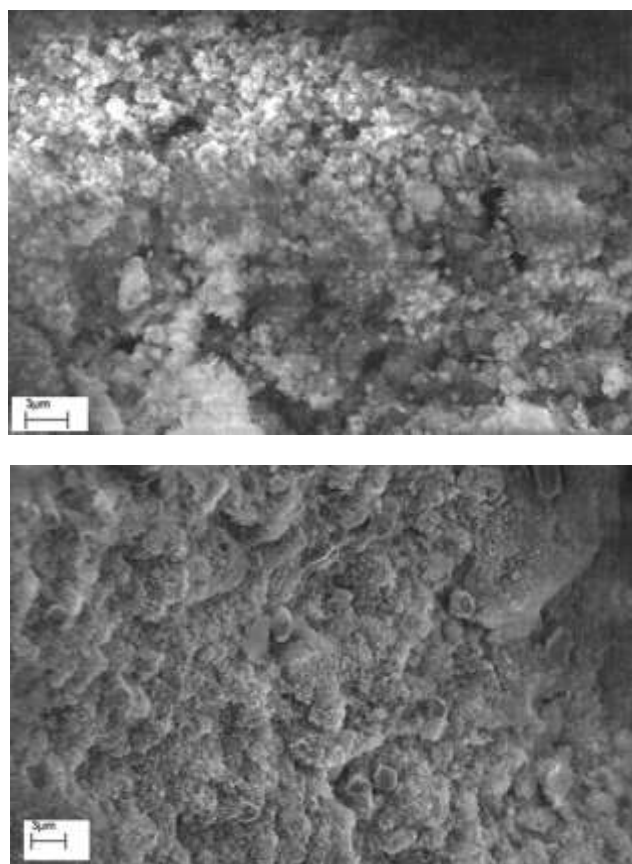


Figure 3: SEM photograph of Co(II)-MCM-41 (top) and Ni(II)-MCM-41 (bottom).

3.1.5. Thermogravimetric analysis (TGA):

The weight loss suffered by calcined MCM-41, Fe(III)-MCM-41, Co(II)-MCM-41, and Ni(II)-MCM-41 on heating from 323 to 1073 K was found to be only 3.12, 5.42, 7.96 and 5.33 % respectively by thermogravimetric measurement. The materials are thus quite stable thermally. In fact, the thermal stabilities of the transition metal incorporated MCM-41 catalysts in air have been well established by many workers using thermogravimetric-differential thermal analysis [32].

3.1.6. Nitrogen adsorption measurements:

The data on BET surface area, pore diameter and pore volume of the catalysts are presented in Table 1. N_2 adsorption-desorption isotherms, pore diameter and relative pore volume plots are shown in Figures 4 and 5. The isotherms belonged to the type IV according to the IUPAC convention and are typical of mesoporous materials [33, 34]. There were no obvious differences in the shapes of the isotherms of MCM-41 and transition metal incorporated MCM-41, although in the latter case, the adsorption rose much more steeply at relatively low relative pressure. However, a large decrease in BET surface area from 1064 to 566, 680 and 801 $m^2 g^{-1}$ was observed due to impregnation of MCM-41 with Fe(III), Co(II) and Ni(II). The decrease in surface area was the highest in case of Fe(III)-MCM-41 (C1) and the lowest in case of Ni(II)-MCM-41 (C3). This indicates that although the amount of Fe(III) entering into MCM-41 was the lowest among all the cations (in this work), the trivalent Fe(III) of relatively small ionic size had the largest influence on the overall surface area. This may be due to various reasons- one of them being the blocking of the pores by the smaller Fe(III) ions to N_2 adsorption resulting in large surface area decrease. Reduction in the mesoporous diameter was observed from 35.4 (MCM-41) to 32.2, 30.1 and 32.2 Å for Fe(III)-MCM-41, Co(II)-MCM-41 and Ni(II)-MCM-41. A decrease in pore volume from 0.942 (MCM-41) to 0.456, 0.512 and 0.645 $cm^3 g^{-1}$ (Table 1) was also observed respectively for Fe(III)-MCM-41, Co(II)-MCM-41 and Ni(II)-MCM-41.

Table 1: Surface and pore characteristics of calcined MCM-41, Fe(III)-MCM-41 (C1), Co(II)-MCM-41 (C2)

and Ni(II)-MCM-41 (C3).

Compound	BJH Pore diameter Å	Total Pore volume cm ³ g ⁻¹	BET surface area m ² g ⁻¹
MCM41	35.4	0.942	1064
Fe(III)-MCM41	32.2	0.456	566
Co(II)-MCM41	30.1	0.512	680
Ni(II)-MCM41	32.2	0.645	801

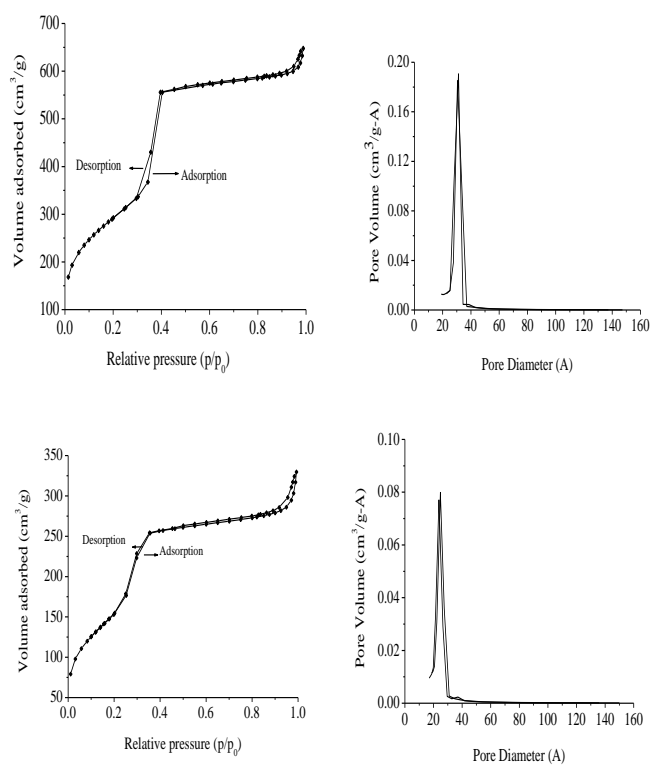


Figure 4: N₂ Adsorption-desorption isotherm and pore diameter and relative pore volume curves of calcined. MCM-41(top) and Fe(III)-MCM-41 (bottom).

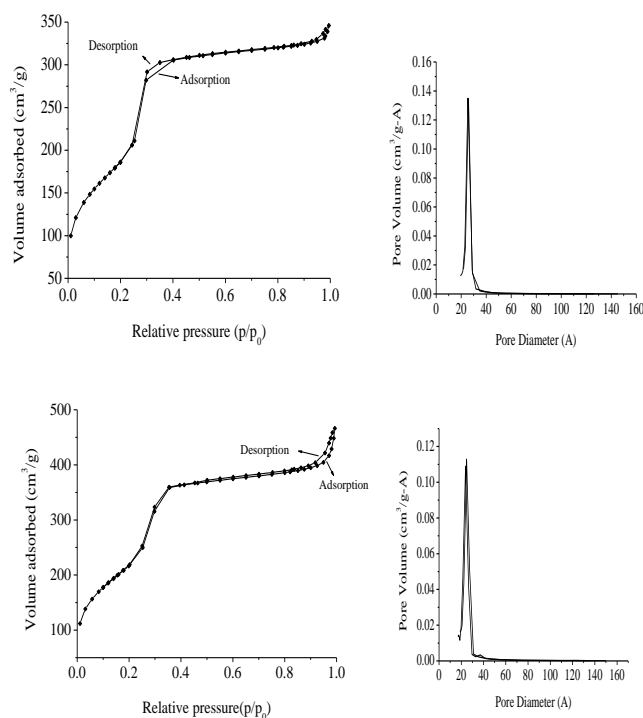


Figure 5. N₂ Adsorption-desorption isotherm and pore diameter and relative pore volume curves of Co(II)-MCM-41 (top) and Ni(II)-MCM-41 (bottom).

3.1.7. Cation exchange capacity (CEC):

The calcined MCM-41 has a CEC of 0.205 m_{eq} g⁻¹. The CEC is affected by metal incorporation into MCM-41 and it is seen that the CEC of Fe(III)-MCM-41 (C1), Co(II)-MCM-41 (C2) and Ni(II)-MCM-41 (C3) increased to 0.255, 0.242 and 0.260 m_{eq} g⁻¹. The CECs of the metal-incorporated MCM-41 differ from one another by an appreciable amount and the difference is quite significant when compared to the CEC of the parent MCM-41. The ion exchange capacity is usually attributed to structural defects, broken bonds and structural hydroxyl transfers [35] and the CEC data indicate that cation incorporation enhances these.

3.2. Adsorption experiment:

A series of experiments was conducted to study adsorption of 2-nitrophenol on the catalysts, Fe(III)-MCM-41 (C1), Co(II)-MCM-41 (C2) and Ni(II)-MCM-41 (C3) at 353 K. Use of Langmuir isotherm (plots of C_e/q_e vs. q_e) yielded a monolayer capacity, q_m of 6.6, 9.3, and 14.1 mg g⁻¹ for the catalysts C1, C2 and C3 respectively. The Langmuir 'b' coefficient had values of 0.022, 0.027 and 0.048 L mg⁻¹ respectively for C1, C2 and C3, indicating a good potential for the formation of 2NP-catalyst adsorption complex. The amount adsorbed was released, when the catalysts with the adsorbates were shaken with water at the same temperature for 1 h. The monolayer capacities indicate that a considerable amount of 2-nitrophenol is held reversibly by adsorption on the catalyst surface and thus, fulfilling the necessary condition for undergoing subsequent oxidation on the catalyst surface. The reversible adsorption is not only advantageous for catalytic conversion of 2-NP, but also makes it possible to easily separate the catalyst after the reaction is over and to reuse the same after drying and other necessary treatment.

3.3. Oxidation of 2-NP:

Oxidation of 2-NP in water has been taken as a model reaction to study the effectiveness of Fe(III)-MCM-41, Co(II)-MCM-41 and Ni(II)-MCM-41 as catalysts. The reaction was carried out under different sets of conditions with the following results.

3.3.1. Blank Experiments:

A set of blank experiments were carried out as follows:

1. Air oxidation of aqueous 2-nitrophenol (10^{-3} mole L^{-1}) on standing when no catalyst and oxidant (H_2O_2) were present in the system,
2. 2-nitrophenol (10^{-3} mole L^{-1}) oxidation by H_2O_2 (1:1 molar ratio) without any catalyst,
3. Oxidation of 2-nitrophenol (10^{-3} mole L^{-1}) by MCM-41 ($2\text{ g } L^{-1}$) alone without any other reactant present in the mixture, and
4. 2-nitrophenol (10^{-3} mole L^{-1}) oxidation when both H_2O_2 (1:1 molar ratio) and MCM-41 ($2\text{ g } L^{-1}$) were present without any transition metal component.

The above blank experiments were carried out under the conditions: temperature 353 K, autogenous pressure 0.2 M^{Pa} , stirrer speed 180 rpm and time interval 5 h. The results did not indicate any measurable conversion in cases (i) and (iii), although conversion to the extent of 3.0 % and 5.4 % respectively, in cases (ii) and (iv) was observed. The conversion, however, could be considered as insignificant compared to those obtained in the reactions described below. The conclusions that can be drawn from these experiments are: (a) aqueous solution of 2-NP neither shows any measurable oxidation in air [as in (i)] or in contact with MCM-41 [as in (iii)], and (b) it is also nearly indestructible either by H_2O_2 [as in (ii)] alone or by H_2O_2 and MCM-41 [as in (iv)]. Further, MCM-41 alone cannot catalyze oxidation of 2-NP. Only when transition metals are incorporated into MCM-41 materials, they become active oxidizing catalysts as demonstrated later.

3.3.2. Effect of reaction time and kinetics:

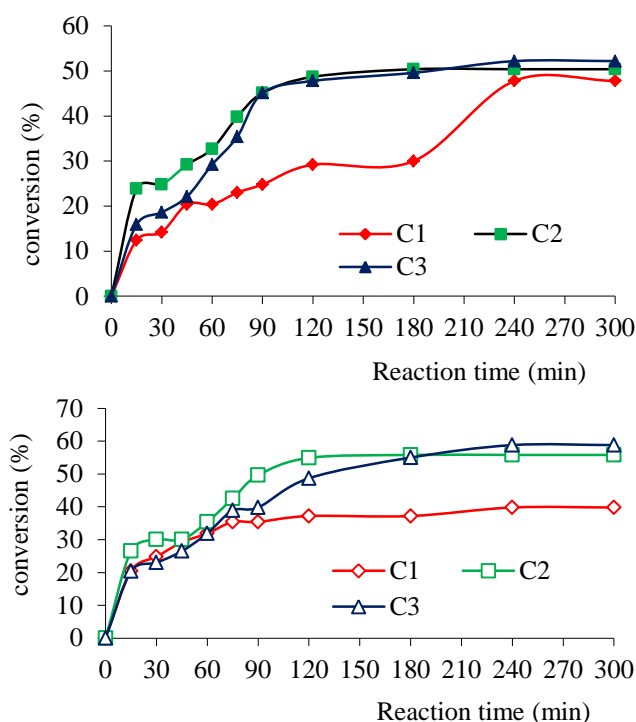


Figure 6: Effects of reaction time on oxidation of 2-nitrophenol with C1, C2 and C3, as the catalysts in presence of H_2O_2 (top) and in absence of H_2O_2 (bottom) at 353 K with catalyst load of $2\text{ g } L^{-1}$, reactant and H_2O_2 concentration of 10^{-3} M , pH for 2-nitrophenol : 5.2.

The oxidation increased from 12.4 to 47.8 % for Fe(III)-MCM-41, 23.9 to 50.4 % for Co(II)-MCM-41 and 15.9 to 52.2 % for Ni(II)-MCM-41 (Figure 6) in the time interval 15 to 300 min (2-NP: H_2O_2 mole ratio 1:1, catalyst load $2\text{ g } L^{-1}$). Interestingly, even with a reaction time of 15 min, Co(II)-MCM-41 could oxidize 23.9 % of 2-NP. The catalysts possessed almost similar efficiency even without the oxidizing agent, H_2O_2 . Thus, the catalysts Fe(III)-MCM-41, Co(II)-MCM-41, and Ni(II)-MCM-41 brought about conversion of 20.4-39.8 %, 26.5-55.8 % and 20.4-58.8 %, respectively (Figure 6) in the same time interval of 15 to 300 min. Significantly, Co(II)-MCM-41 and Ni(II)-MCM-41 converted more 2-NP in 300 min when no H_2O_2 was present. Conversion reached near equilibrium at 180 min for Co(II)-MCM-41, and 240 min for Fe(III) and Ni(II) supported MCM-

41. Luo et al. [19] have found 42.8 % conversion of styrene with dilute hydrogen peroxide (H₂O₂, 30 wt%) over Ti-MCM-41 catalyst in 180 min indicating the transition metal ions as the active sites for oxidation. Compared to these results, the present work has achieved 58.8 % conversion of 2-NP with Ni(II)-MCM-41 even without an oxidizing agent in an equilibrium time of 240 min.

Applying first order kinetics to 2-NP oxidation, according to the equation:

$$C_t = C_o \exp(-kt)$$

$$\text{Or, } \log C_t = \log C_o - (k/2.303) t$$

(C_o and C_t are the concentrations of 2-NP at commencement of the oxidation (t = 0) and at any time, t, and k is the first order rate coefficient) and plotting log C_t vs. t, good linear plots (Figure 7) are obtained, both in presence of H₂O₂ (R = - 0.97), and in absence of H₂O₂ (R = - 0.98 to - 0.99). The rate coefficient had values of 2.3 x 10⁻³ min⁻¹, 3.7 x 10⁻³ min⁻¹ and 3.9 x 10⁻³ min⁻¹ (with H₂O₂) and 4.8 x 10⁻³, 4.8 x 10⁻³ and 4.4 x 10⁻³ min⁻¹ (without H₂O₂) for Fe(III), Co(II) and Ni(II) anchored MCM-41, respectively. Among the catalysts, it is observed that Ni(II)-MCM-41 in presence of H₂O₂ and Co(II)-MCM-41 in absence of H₂O₂ brings about faster conversion of 2-NP. Egerton et al. [10] have observed first order kinetics for the photocatalytic oxidation of 2-nitrophenol and 4-nitrophenol over titanium dioxide. Liquid-phase oxidation of phenol has also been shown by Stoyanova et al. [36] to proceed with first-order kinetics with a rate coefficient of 2 x 10⁻² min⁻¹ at 308 K with pH 6.0 and catalyst (mixed Ni-Mn oxide) load of 0.5 g L⁻¹.

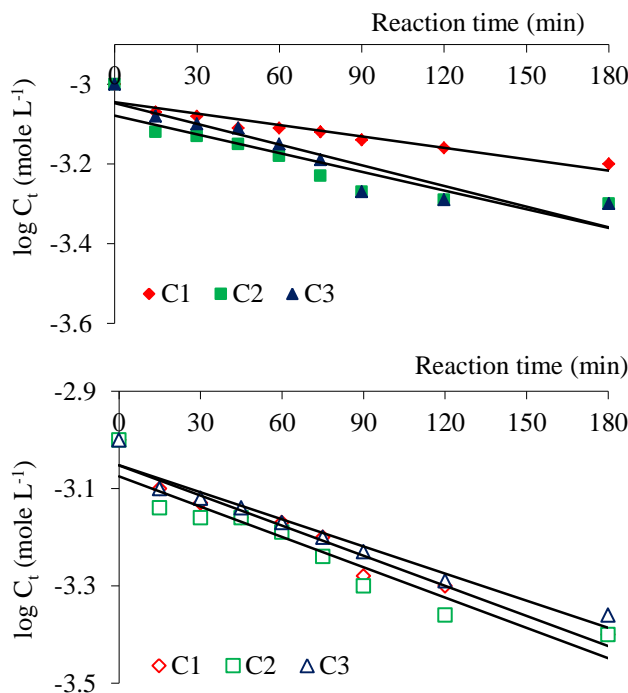
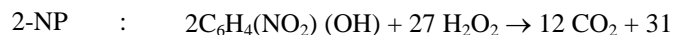


Figure 7: First-order degradation of 2-nitrophenol (10⁻³ M) by wet oxidation in presence of H₂O₂ (top) and in absence of H₂O₂ (bottom) over C1, C2 and C3 at 353 K [catalyst load 2 g L⁻¹; reactant: H₂O₂ mole ratio 1:1].

3.3.3. Effects of mole ratio:

An increase in the mole ratio of hydrogen peroxide and 2-nitrophenol from 1:1 to 20:1 for a fixed reaction time of 300 min (catalyst load 2 g L⁻¹) had very little effect on the conversion. There was only marginal changes, e.g. from 47.8 to 48.5 % for Fe(III)-MCM-41 (C1), 50.4 to 52.0 % for Co(II)-MCM-41 (C2) and 52.2 to 55.1 % for Ni(II)-MCM-41 (C3) in the same range of reactants composition. 1:1 mole ratio of the reactant to the oxidant is all that is needed for achieving a considerable destruction of 2-nitrophenol. Even when a large excess of H₂O₂ was in the reaction mixture, it was likely that more and more H₂O₂ underwent self-decomposition instead of oxidizing 2-NP. The decomposition must have been helped by the presence of the catalyst. It is interesting to note that the complete oxidation of 2-nitrophenol (2-NP) requires 27/2 moles of H₂O₂ as found from the stoichiometric equation:





The results show that such stoichiometry may be valid for homogeneous 2-NP oxidation, but does not hold good for the catalytic oxidation. The conversion increased (although not remarkably) from 2-NP: H₂O₂ mole ratio of 1:1 to 1:15 for C1 and from 1:1 to 1:10 for C2 and C3 and any further increase in the mole ratio did not have any observable effect.

3.3.4. Effects of catalyst load:

At the lowest catalyst load of 2 g L⁻¹, Fe(III)-MCM-41 could convert 47.8 % of 2-NP in presence of H₂O₂ compared to 50.4 % for Co(II)-MCM-41 and 52.2 % for Ni(II)-MCM-41. When the catalyst load is increased to 10 g L⁻¹, the conversion remained constant for Co(II)-MCM-41 (50.4 %) and changed marginally to 48.0 and 55.0 % for Fe(III) and Ni(II) immobilized MCM-41. Under the same set of conditions, but without taking H₂O₂ in the reactant feed, increased conversion was observed with all the three catalysts from 39.8-41.5 % for Fe(III)-MCM-41, 55.8-58.4 % for Co(II)-MCM-41 and 58.8-60.5 % for Ni(II)-MCM-41 corresponding to an increase in catalyst load from 2 to 10 g L⁻¹.

Similar results have been seen from works of other researchers. For example, it is observed in the liquid phase oxidation of phenol under identical conditions (T 308 K, pH 6.0, constant phenol concentration, catalyst mixed Ni-Mn oxide, 0.5 to 10 g L⁻¹), the degree of conversion is ~ 28 % for a load of 0.5 g L⁻¹ and ~ 100 % for a load of 10 g L⁻¹ [36]. In the present work, catalyst loads of > 2 g/L did not bring about significant enhancement in oxidation, and that a load of 2 g L⁻¹ could bring about 50-60 % oxidation of 2-nitrophenol. Considering that 2-nitrophenol is much more resistant to oxidation than phenol, the oxidation achieved in this work is very significant.

3.3.5. Effects of 2-NP concentration:

Oxidation of 2-NP is likely to decline if the concentration of the reactant is increased. Thus, when the concentration of 2-NP was increased from 2 x 10⁻⁴ M to 4 x 10⁻⁴, 6 x 10⁻⁴, 8 x 10⁻⁴ and 10 x 10⁻⁴ M, oxidation declined from 58.2 to 47.8 % for Fe(III)-MCM-41, 60.6 to 50.4 % for Co(II)-MCM-41 and 66.2 to 52.2 % for Ni(II)-MCM-41 with H₂O₂ and 55.0 to 39.8 %, 64.5 to 52.3 % and 68.2 to 58.8 % for Fe(III), Co(II) and Ni(II) supported MCM-41 without H₂O₂ (Figure 8). With increase in concentration, more and more molecules of 2-nitrophenol would be competing for the catalyst sites and the fraction of the molecules undergoing oxidative decomposition came down, although the net conversion might still increase.

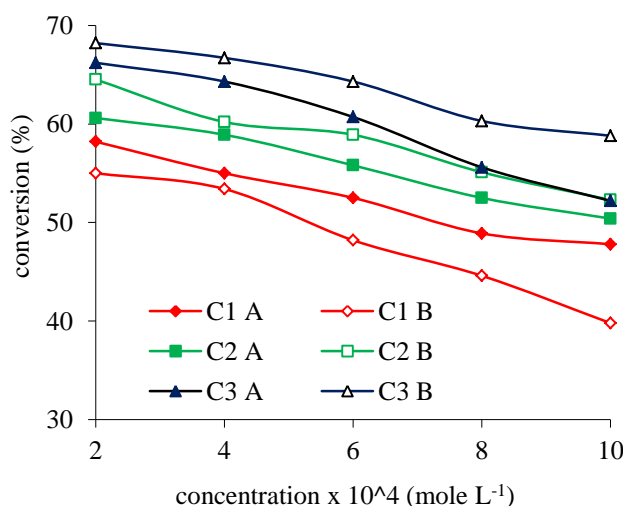


Figure 8: Effects of 2-nitrophenol concentration on its catalytic wet oxidation at 353 K and reaction time of 300 min in presence (A) of H₂O₂ (2 x 10⁻⁴ mole L⁻¹) and in absence (B) of H₂O₂.

3.3.6. Effects of temperature:

More and more 2-nitrophenol underwent degradation with increase in reaction temperature from 303 to 413 K

(Figure 9). The increase in conversion were 45.3 to 53.7 % for Fe(III)-MCM-41 (C1), 48.9 to 65.1 % for Co(II)-MCM-41 (C2) and 50.9 to 58.7 % for Ni(II)-MCM-41 (C3) in presence of H₂O₂ and from 36.0 to 54.9 % (C1), 49.0 to 70.0 % (C2), 52.0 to 74.3 % (C3) without H₂O₂.

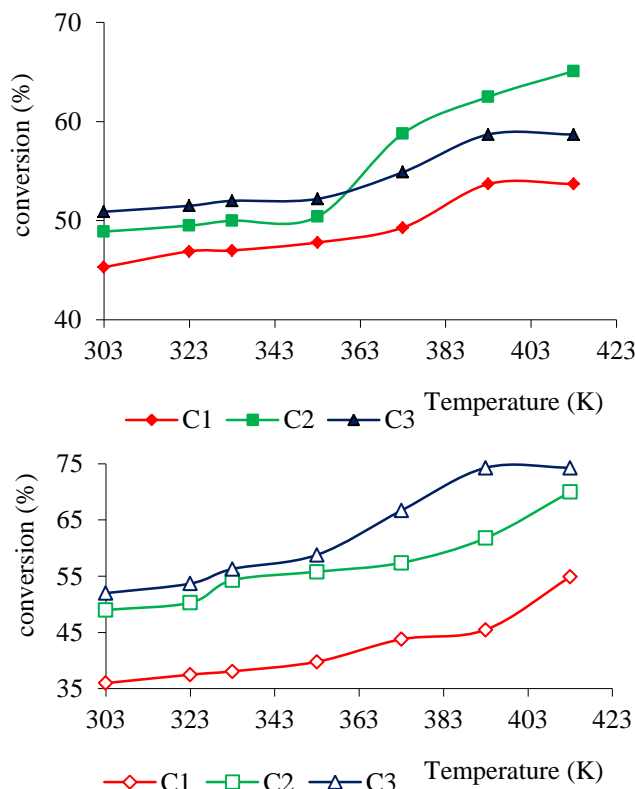


Figure 9: Effects of temperature on oxidation of 2-nitrophenol (Initial concentration 10⁻³ M) with C1, C2 and C3 as the catalysts in presence (top) and in absence (bottom) of H₂O₂ (Reaction time 300 min, catalyst load 2 g L⁻¹, H₂O₂ concentration 10⁻³ M).

With increase in temperature, the collision frequency of 2-NP molecules in solution increases and as a result, the possibility of oxidation increases and the conversion improves. However, as the temperature increases the adsorption of 2-NP molecules on the catalyst surface is likely to decrease and therefore, the increase in conversion is not as large as expected.

3.3.7. Effects of pH:

Influence of pH on 2-nitrophenol oxidation was studied from pH 3.0 to 9.0. The conversion increased from 45.2 to 62.1 % for Fe(III)-MCM-41 (C1), 48.6 to 69.0 % for Co(II)-MCM-41 (C2) and 48.9 to 62.3 % for Ni(II)-MCM-41 (C3), when H₂O₂ was present. When the oxidation was carried out without H₂O₂, the increase in conversion in the pH range of 3.0 to 9.0 was from 37.6 to 59.8 % (C1), 52.3 to 72.1 % (C2) and 55.6 to 69.4 % (C3). At the natural pH of aqueous 2-nitrophenol solution (pH 5.2), the conversion was: 47.8 % with H₂O₂ and 39.8 % without H₂O₂ for C1; 50.4 and 55.8 % for C2, 52.2 and 58.8 % for C3. Under the presence and in the absence of H₂O₂, the oxidation of 2-NP increases with the increase in pH for all the catalysts. It is seen from Figure 10 that for the catalysts, C2 and C3, the conversion was more when no H₂O₂ was present at the same pH. The situation was reverse for C1.

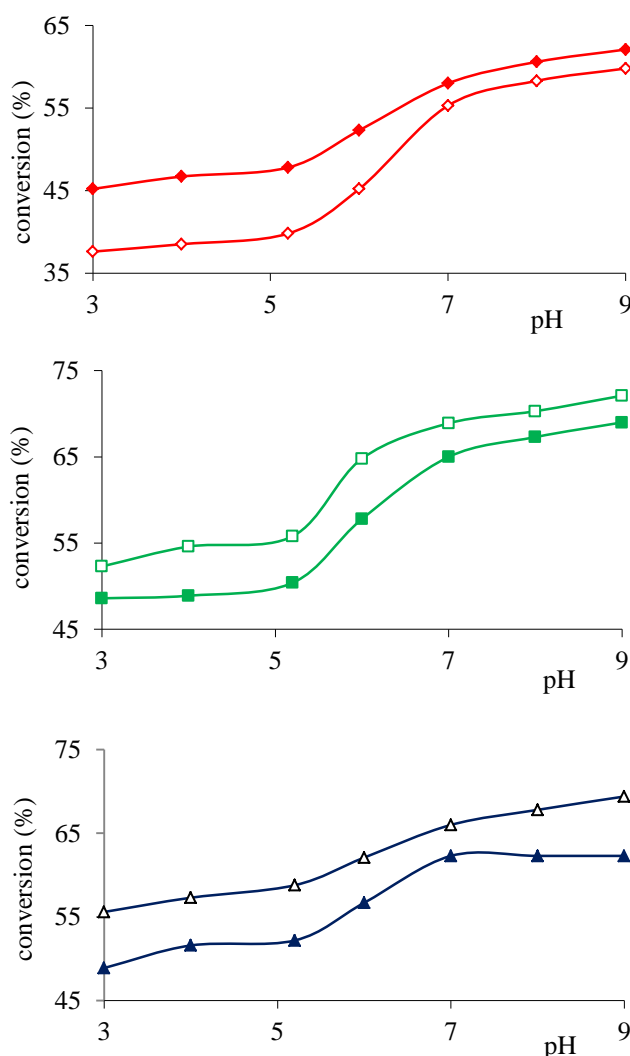


Figure 10: Effects of pH on oxidation of 2-nitrophenol over C1 (top), C2 (middle) and C3 (bottom) at 353 K with H₂O₂ (filled symbols) and without H₂O₂ (open symbols) (2-nitrophenol 10⁻³ M, time 300 min, catalyst load 2 g L⁻¹, reactant: H₂O₂ mole ratio 1:1).

Egerton et al. [10] have shown that if the pH was increased from 5.2 to 5.8 in the photocatalytic oxidation of 2-nitrophenol by TiO₂, the degradation rate of 2-NP rose by ~70 %, but for a further increase from 5.8 to 7.7, the degradation increased only marginally (~10 %). These results are reasonably consistent with the conclusion of Wang et al. [37] that pH 7 is the optimum one for oxidation of nitrophenols, but are contrary to the general decrease in rate with increasing pH observed by Augugliarno et al. [38]. The contradictory results of the two groups of workers might be due to the differences in the catalyst material since two different varieties of TiO₂ were used.

Although no comparable report in relation to the present work could be found, it is obvious that increase in H⁺ ions does not favour 2-NP oxidation. This may be due to the fact that with more H⁺ ions in solution, the bulky 2-NP molecules have to compete with the same for adsorption sites on the catalyst surface and obviously, H⁺ ions have a higher affinity for the catalyst surface than do the 2-NP molecules.

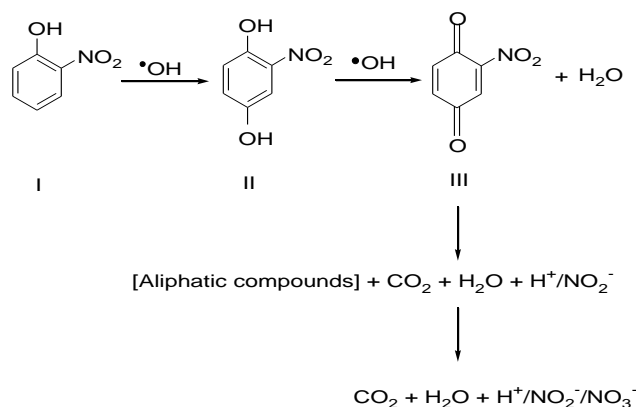
3.3.8. Mechanistic consideration:

A mechanism for the oxidation of 2-NP is suggested below based on (i) GC-MS identification of some products after the reaction, (ii) known products of degradation obtained from literature and (iii) possible products of degradation from the knowledge of degradation pathways likely to be followed by the reactants. In GC-MS analysis, (i) 2-nitrohydroquinone and (ii) 2-nitro-1,4-benzoquinone were found in the product mixture of 2-NP

oxidation.

The probable pathway for oxidation of 2-NP (I) initiated by the catalysts could be proposed to have preceded via the hydroxyl radicals (Scheme 1) as follows:

1. The radicals will add to 2-NP (I) at the para-position of the cyclic ring to give 2-nitrohydroquinone (II),
2. This product (II) is converted by more hydroxyl radicals to 2-nitro-1,4-benzoquinone (III),
3. 2-nitro-1,4-benzoquinone (III) undergoes further transformation through ring cleavage and subsequent degradation to simple aliphatic compounds, which will eventually decompose to CO_2 , H_2O , HNO_2 and HNO_3 [39].



Scheme 1: Degradation pathway of 2-nitrophenol.

Najjar et al. [39] have suggested an identical scheme for degradation of 2-NP by photo-degradation on Al-pillared montmorillonite doped with copper.

4. Conclusion:

The results show that introduction of the transition metals, Fe(III), Co(II) and Ni(II) anchored MCM-41 through the simple process of impregnation could give very active and effective catalysts for wet oxidation of 2-nitrophenol. These catalysts can bring about wet oxidation of 2-NP even without the presence of an oxidizing agent like hydrogen peroxide and in many cases, the results are better than those in the presence of the oxidizing agent.

Like most of the organic compounds 2-NP oxidation also follows first order reaction kinetics satisfactorily. The main advantage of the present work is that 2-nitrophenol could be oxidized to 2-nitrohydroquinone and 2-nitro-1,4-benzoquinone which further decomposed to CO_2 , H_2O , HNO_2 , and HNO_3 .

Acknowledgments:

This work was supported by Gauhati University (India) research fund, Dongguk University, Gyeongju research fund and Marwadi University, Rajkot, Gujarat.

References:

- [1] Arana J. et al., "Highly Concentrated Phenolic Wastewater Treatment by Heterogeneous and Homogeneous Photocatalysis: Mechanism Study by FTIR-ATR." *Water Sc. Technol.* 44 (2001): 229-236.
- [2] Shi et al. "Synthesis of $\text{CoFe}_2\text{O}_4/\text{MCM-41}/\text{TiO}_2$ composite microspheres and its performance in degradation of phenol" *Mat Sci Semicon Proc.* 37(2015): 241-249.
- [3] Busca G., Berardinelli S., Resini C., and Arrighi L., "Technologies for the removal of phenol from fluid streams: a short review of recent developments". *J. Hazard. Mater.* 160 (2008): 265-288.
- [4] Jiang S., Zhang H., and Yan Y., "Catalytic wet peroxide oxidation of phenol wastewater over a novel Cu-ZSM-5 membrane catalyst". *Catal. Comm.* 71 (2015): 28-31.
- [5] Agency for Toxic Substances and Disease Registry (ATSDR). 1992. Toxicological Profile for nitrophenols. Atlanta, GA: U.S. Department of Health and Human Services, Public Health Service.



- [6] Ribeiro R. S. et al. "Removal of 2-nitrophenol by catalytic wet peroxide oxidation using carbon materials with different morphological and chemical properties". *App. Catal. B: Environ.* 140-141 (2013): 356-362.
- [7] Shaoqing Y., Jun H., and Jianlong W., "Radiation-induced catalytic degradation of p-nitrophenol (PNP) in the presence of TiO₂ nanoparticles" *Radiat. Phys. Chem.* 79 (2010): 1039-1046.
- [8] Rehman S., Siddiq Md., Al-Lohedan H., Sahiner N., "Cationic microgels embedding metal nanoparticles in the reduction of dyes and nitro-phenols". *Chem. Eng. J.* 265 (2015): 201-209.
- [9] Rabaaoui N. et al. "Anodic oxidation of o-nitrophenol on BDD electrode: variable effects and mechanisms of degradation". *J. Hazard. Mater.* 250-251 (2013): 447-453.
- [10] Egerton, T.A. et al. "The effect of UV absorption on the photocatalytic oxidation of 2-nitrophenol and 4-nitrophenol". *J. App. Electrochem.* 35 (2005): 799-813.
- [11] Legrini O., Oliveros E., and Braun A.M., "Photochemical processes for water treatment", *Chem. Rev.* 93(2) (1993): 671-698.
- [12] Preis S., Kamanev S., Kallas J., and Munter R., "Advanced oxidation processes against phenolic compounds in wastewater treatment". *Ozone Sci. Eng.* 17(1995): 399-419.
- [13] Andreozzi R., Caprio V., Insola A., and Marotta R., "Advanced oxidation processes (AOP) for water purification and recovery". *Catal. Today.* 53(1999): 51-59.
- [14] Dzengel J., Theurich J., and Bahnemann D.W. "Formation of nitro aromatic compounds in advanced oxidation processes: photolysis versus photocatalysis" *Environ. Sci. Technol.* 33(1999): 294-300.
- [15] Ilisz, I. et al. "Removal of 2-chlorophenol from water by adsorption combined with TiO₂ photocatalysis", *App. Catal. B: Environ.* 39 (2002): 247-256.
- [16] Doong, R.A.; Maithreepala, R.A.; and Chang, S.M. "Heterogeneous and homogeneous photocatalytic degradation of chlorophenols in aqueous titanium dioxide and ferrous ion", *Water Sc. Technol.* 42 (2000): 253-260.
- [17] Pignatello J.J., Oliveros E., and MacKay A. "Advanced oxidation processes for organic contaminant destruction based on the Fenton reaction and related chemistry". *Crit Rev Env. Sci Tec.* 36(2006): 1-84.
- [18] Kresge C.T. et al. "Ordered mesoporous molecular sieves synthesized by a liquid-crystal template mechanism", *Nature*, 359 (1992): 710-712.
- [19] Luo Y., Lu G.Z., Guo Y.L, and Wang Y.S. "Study on Ti-MCM-41 zeolites prepared with ... characterization and catalysis". *Catal. Comm.* 3(2002): 129-134.
- [20] Yang F et al. "Coordination of manganese porphyrins on amino-functionalized MCM-41 for heterogeneous catalysis of naphthalene hydroxylation Chinese" *J. Catal.* 36(2015): 1035-1041.
- [21] Zhou J. et al., MCM-41 supported aminopropylsiloxane palladium(0) complex: a highly active and stereoselective catalyst for Heck reaction *J. Mol. Catal. A: Chem.* 178(2002): 289-292.
- [22] Srinivas, N. et al. "Liquid phase oxidation of anthracene and trans-stilbene over modified mesoporous (MCM-41) molecular sieves", *J. Mol.Catal. A: Chem.* 179 (2002): 221-231.
- [23] Chen D. et al., "Effect of oxygen pretreatment on the surface catalytic oxidation of HCHO on Ag/MCM-41 catalysts", *J. Mol Catal. A: Chem.* 404-405 (2015): 98-105.
- [24] Beck, J.S. et al. "A new family of mesoporous molecular sieves prepared with liquid crystal templates", *J. Am. Chem. Soc.* 114 (1992): 10834-10843.
- [25] Bergaya, F.; and Vayer, M. "CEC of clays: Measurement by adsorption of a copper ethylenediamine complex", *App. Clay Sc.* 12 (1997): 275-280.
- [26] Liepold, A. et al. "Textural, structural and acid properties of a catalytically active mesoporous aluminosilicate MCM-41" *J. Chem. Soc. Faraday Trans.* 92 (1996): 4623-4629.
- [27] Wu et al. "Synthesis, characterization and catalytic performance for phenol hydroxylation of Fe-MCM41 with high iron content". *Micropor Mesopor Mater.* 113(2008): 163-170.
- [28] Qi F., Chu W., and Xu B. "Modeling the heterogeneous peroxymonosulfate/Co-MCM41 process for the degradation of caffeine and the study of influence of cobalt sources". *Chem. Eng. J.* 235 (2014): 10-18.
- [29] Jung J-S. et al., "Synthesis and characterization of Ni magnetic nanoparticles in AIMCM41 host". *J. Phys. Chem. Solids*, 64 (2003): 385-390.
- [30] S. Schwarz, D. R. Corbin, A. J Vega, In R.F. Lobo, J.S. Beck, S.L. Suib, D.R. Corbin, M.E. Davis, L.E. Iton, S.I. Zones (Eds.) (1996). *Materials Research Society Symposium Proceedings*, Materials Research Society, Pittsburg, PA, Vol. 431, p. 137.
- [31] Koh, C.A.; Nooney, R.; and Tahir, S. "Characterisation and catalytic properties of MCM-41 and Pd/MCM-41 materials". *Catal. Letter*, 47 (1997): 199-203.
- [32] Selvaraj, M. et al. "Synthesis and characterization of Mn-MCM-41 and Zr-Mn-MCM-41". *Microporous Mesoporous Mater.* 78 (2005): 139-149.
- [33] Zheng, S. et al. "Synthesis, characterization and photocatalytic properties of titania-modified mesoporous silicate MCM-41". *J. Mater. Chem.* 10 (2000): 723-727.



- [34] Shylesh, S.; and Singh, A.P. "Vanadium containing ordered mesoporous silicates: Does the silica source really affect the catalytic activity, structural stability, and nature of vanadium sites in V-MCM-41". *J. Catal.* 233 (2005): 359-371.
- [35] Rodrigues, M.G.F. "Physical and catalytic characterization of smectites from Boa-Vista, Paraiba, Brazil. *Ceramica.* 49 (2003): 146-150.
- [36] Stoyanova, M.; Christoskova, St.; and Georgieva, M. "Mixed Ni-Mn-oxide systems as catalysts for complete oxidation: Part II. Kinetic study of liquid-phase oxidation of phenol", *App. Catal. A: General.* 249 (2003): 295-302.
- [37] Wang K.H., Hsieh Y.H., and Chen L.J., "The heterogeneous photocatalytic degradation intermediates and mineralization for the aqueous solutions of cresols and nitrophenols". *J. Hazard. Mater.* 59(1998): 251-260.
- [38] Augugliaro, V. et al. "Photocatalytic degradation of nitrophenols in aqueous titanium dioxide dispersion". *App. Catal.* 69 (1991): 323-340.
- [39] Najjar W., Chirchi L., Santos E., and Ghorhel A. "Kinetic study of 2-nitrophenol photodegradation on Al-pillared montmorillonite doped with copper" *J. Environ. Monitoring.* 3(6) (2001): 697-701.